iScience

CellPress
OPEN ACCESS

Article

Regenerable temperature-responsive biocatalytic nanofiltration membrane for organic micropollutants removal

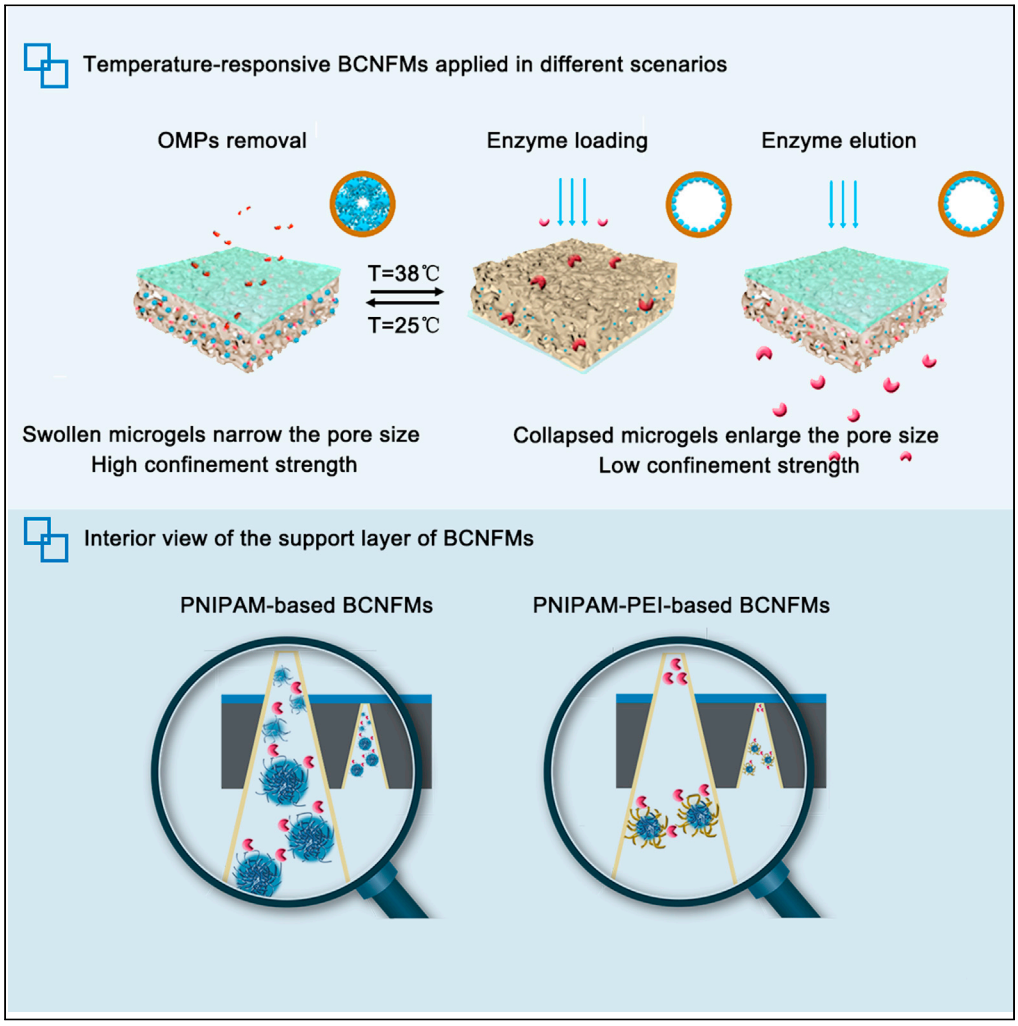

Hao Zhang, Jianquan Luo, Yinhua Wan

jqluo@ipe.ac.cn (J.L.)
yhwan@ipe.ac.cn (Y.W.)

Highlights

PNIPAM modification increases the geometric confinement of support layer to laccase

PNIPAM-based BCNFMs exhibit temperature-responsive reversible nanogating function

PNIPAM-based BCNFMs show high BPA removal efficiency and long-term stability

PNIPAM-PEI-based BCNFMs can be easily regenerated when operated at 38°C

Zhang et al., iScience *25*, 103671
January 21, 2022
https://doi.org/10.1016/j.isci.2021.103671

iScience

CellPress
OPEN ACCESS

Article

Regenerable temperature-responsive biocatalytic nanofiltration membrane for organic micropollutants removal

Hao Zhang,[1] Jianquan Luo,[1,2,*] and Yinhua Wan[1,*]

SUMMARY

Biocatalytic nanofiltration membranes (BNMs) exhibit great potentials in organic micropollutants removal attributed to its synergistic effect between enzyme catalysis and membrane separation. However, the difficulties in regeneration of the BNMs halted their economic practicality. Inspired by cell membranes with stimuli-responsive channels, we have developed the temperature-responsive BNMs with nanogating function by poly(N-isopropyl acrylamide) (PNIPAM) modification. PNIPAM modification increases the geometric confinement of the support layer to enzymes, thus improving enzyme loading, inhibiting enzyme leakage, and preventing membrane permeability decline caused by enzyme excess migration and aggregation. By optimizing the concentration of reaction monomers, modification time, and strategies, the PNIPAM-based BNMs show high bisphenol A (BPA) removal efficiency and long-term stability. Furthermore, the PNIPAM-polyethyleneimine-based BNMs can be easily regenerated at 38°C, and the laccase activity and BPA removal efficiency are fully recovered. This work would promote the real application of BNMs in bioconversion, drug delivery, and biosensors.

INTRODUCTION

Organic micropollutants (OMPs), such as endocrine disrupters, pesticides, pharmaceuticals, and personal care products, have attracted increasing attention owing to their detrimental effects on human health even at trace levels (Ma et al., 2018; Roman et al., 2021). Most of the OMPs have low molecular weight, high chemical resistance, and ultra-low concentration, which make them hard to remove or degrade by traditional wastewater treatment methods (Grandclement et al., 2017). Enzymes are green and sustainable catalysts with outstanding catalytic efficiency on OMPs degradation (Varga et al., 2019). However, the fragile nature and soluble property of the enzyme lead to poor stability and recyclability, thereby hindering its large-scale industrial application (Sha et al., 2021). Membrane filtration is also one of the most attractive methods to remove OMPs (Liu et al., 2019b). However, it still suffers from a low retention rate even using reverse osmosis (RO) membrane as some of the OMPs would pass through the membrane by the solution-diffusion pathway (Yoon et al., 2006).

In the light of good biocompatibility, low cost, and easy functionalization, the membrane is regarded as one of the most attractive immobilization supports for better enzyme reuse. Therefore, many researchers have devoted studies to developing biocatalytic membranes by immobilizing enzymes in/on the membrane for OMPs removal (Cen et al., 2019; Jochems et al., 2011; Zdarta et al., 2019). Enzymes immobilized in/on the membrane can not only increase their stability and reusability but also endow the membrane with catalytic function, thereby alleviating membrane fouling and adsorption saturation caused by OMPs (Barbhuiya et al., 2022; Fan et al., 2017). Moreover, compared with the conventional diffusion-controlled biocatalytic processes, biocatalytic membranes can be operated in flow-through mode (convective transport), which accelerates the mass transfer of the substrates and facilitates *in situ* products removal, thus elevating enzyme activity and avoiding products inhibition on the immobilized enzymes (Li et al., 2020; Mazzei et al., 2021). Moreover, combining particles with the membrane can improve the enzyme immobilization process because some desirable particles would provide a favorable microenvironment and increase the immobilization sites of the membrane (Vitola et al., 2017). In recent years, immobilizing enzymes in/on the support layer of nanofiltration (NF) membrane by "reverse filtration" exhibits great advances in OMPs removal (Luo

[1]State Key Laboratory of Biochemical Engineering, Institute of Process Engineering, University of Chinese Academy of Sciences, Chinese Academy of Sciences, Beijing 100190, China

[2]Lead contact

*Correspondence: jqluo@ipe.ac.cn (J.L.), yhwan@ipe.ac.cn (Y.W.)

https://doi.org/10.1016/j.isci.2021.103671

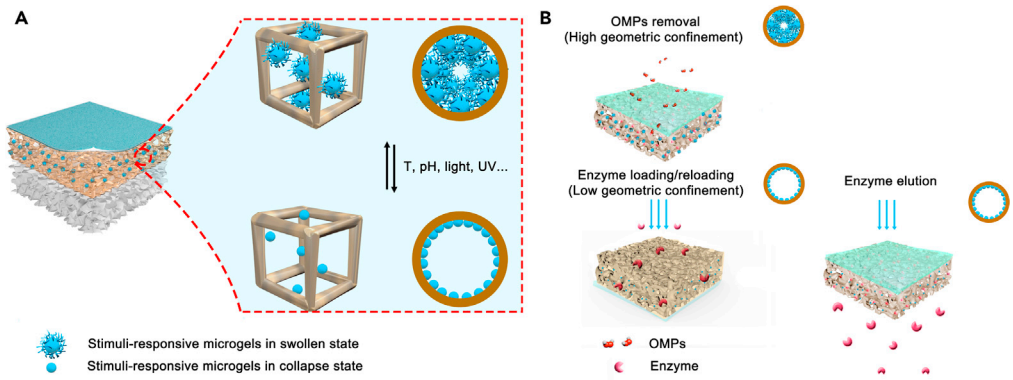

Figure 1. Artificial smart BNMs by incorporating stimuli-responsive microgels into the porous support layer of NF membrane

(A) Schematic diagram of reversible functional gates of the support layer.

(B) Applications of smart BNMs in different operation scenarios.

et al., 2020). Thanks to the large specific surface area of the support layer and the positive synergistic effect between membrane separation and enzyme catalysis, the prepared biocatalytic NF membranes (BNMs) exhibit superior OMPs removal efficiency (Cao et al., 2016). Nevertheless, reverse filtration forces the enzyme to be immobilized into the support layer in a chaotic way that raises the risk of enzyme aggregation and membrane permeability decline (Zhang et al., 2019a). In addition, to prevent enzyme leakage, polydopamine (PDA) coating was used to seal the enzyme inside the NF membrane, and nanomaterials (e.g., graphene oxide and metal-organic frameworks) were introduced into the support layer to adsorb and stabilize the enzyme (Cao et al., 2018; Ren et al., 2018; Zhang et al., 2019b). Despite the low enzyme leakage by the above strategies, the high steric hindrance caused by PDA coating and nanomaterials led to a rigid structure of the immobilized enzyme and severe products accumulation, thereby reducing the enzyme activity and stability. Very recent findings by our group showed that rational design of the confinement strength of the support layer to the enzyme by polyelectrolytes-based three-dimensional modification method could improve the activity and stability of the BNMs (Zhang et al., 2020). However, when the immobilized enzyme is inactivated or the OMPs removal efficiency cannot meet the demands, such BNMs are difficult to regenerate as the confinement strength of the membrane cannot be tuned once the membrane is fabricated.

Inspired by cell membranes with stimuli-responsive channels, we proposed to develop artificial smart BNMs by incorporating stimuli-responsive microgels into the porous support layer of NF membrane as functional gates (Liu et al., 2016, 2019a). The proposed smart BNMs can flexibly and reversibly adjust pore sizes and surface properties of the porous support layer based on the "swelling/collapse" switch of stimuli-responsive microgels (Figure 1A). Moreover, the introduction of stimuli-responsive microgels can increase the geometric confinement and the specific surface areas of the support layer. In this way, such smart BNMs can fit multiple operation scenarios thanks to the large-extent self-regulation of the confinement strength of the support layer to the immobilized enzyme. When the BNMs are used for OMPs removal, we can arrange the microgels in a swollen state, and thus the pores of the support layer would be narrowed, which can effectively prohibit enzyme leakage. When the immobilized enzyme is inactivated, the microgels can be switched into a collapsed state, and the resulting larger pore size of the support layer reduces its geometric confinement to enzymes, thus facilitating the elution of the inactivated enzyme and realizing enzyme reloading (Figure 1B).

There are various types of stimuli-responsive microgels that respond to different external stimuli such as temperature, pH, pressure, ionic strength, specific molecules, and light (Plamper and Richtering, 2017; Qiao et al., 2019; Saad et al., 2020). Considering the fragile and sensitive nature of the enzyme and membrane, we need to choose a type of microgel with mild responsive conditions and ease of operation. Thereinto, temperature-responsive poly(N-isopropylacrylamide) (PNIPAM) microgels attract our attention owing to their pronounced thermal response near physiological temperature (32°C), mature synthesis process, good biocompatibility, and high monodispersity (Nöth et al., 2020; Reinicke et al., 2019; Rey et al., 2020). PNIPAM is hydrophilic and swollen in aqueous media below 32°C, whereas it becomes hydrophobic

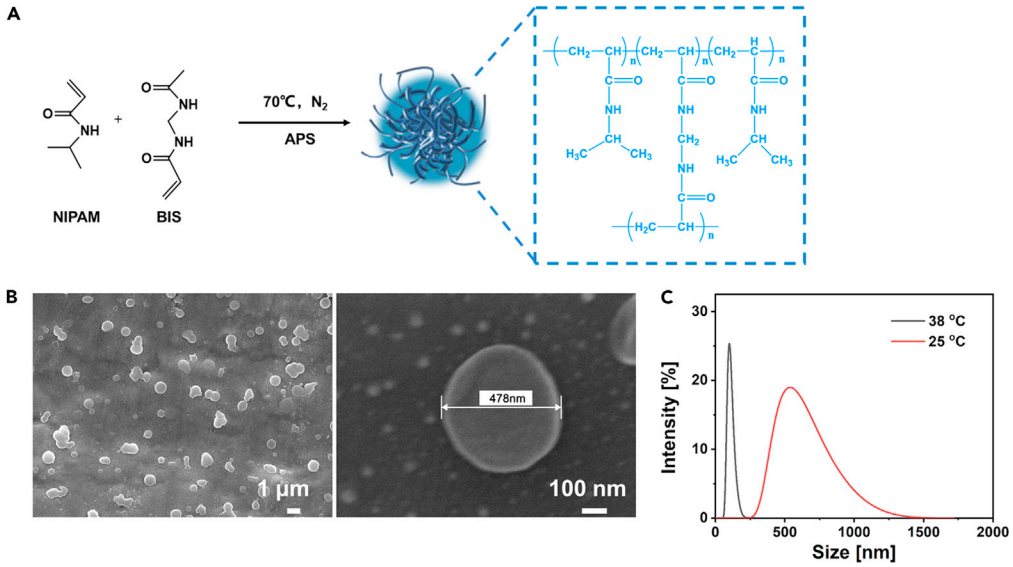

Figure 2. Synthesis and characterization of PNIPAM microgels

(A) Scheme for the synthesis of PNIPAM microgels by precipitation polymerization method.

(B) FESEM images of PNIPAM microgels.

(C) DLS measurement of the size distribution of PNIPAM microgel under 25°C and 38°C, respectively.

and collapsed above 32°C (Xiao et al., 2013). Therefore, when operated at room temperature (25°C), the hydrophilic nature of PNIPAM microgels would provide a desirable microenvironment for enzyme catalysis (Popat et al., 2011).

In this work, laccase, a multi-copper oxidase enzyme, was chosen for preparing BNMs as it can efficiently catalyze the oxidation of phenolic compounds such as bisphenol A (BPA) and chlorophenols (Daronch et al., 2020). The temperature-responsive NF membrane with reversible nanogating function was first developed by *in situ* growth/confinement of PNIPAM microgels and co-deposition of PNIPAM-PEI/PDA in the support layer, respectively. Then, laccase was reversely filtrated into the support layer of the PNIPAM modified NF membrane at 38°C (T > low critical transition temperature [LCST]) for the fabrication of smart BNMs. Herein, the prepared BNMs can be perfectly applied in different operation scenarios as they can substantially self-regulate the confinement strength of the support layer to the immobilized enzyme. The membrane structure and surface property during the preparation were characterized, and the influence of modification conditions including monomers concentration and grafting time was systematically investigated. Moreover, the properties of the smart BNMs (enzyme loading, permeability, BPA removal efficiency) were evaluated. In addition, the effect of enzyme leakage and products accumulation on the stability of the BNMs was discussed. Finally, the regeneration ability of the prepared BNMs was assessed and discussed. To the best of our knowledge, there is no previous study regarding the fabrication of BNMs with nanogating function for OMPs removal. This work offered a new BNMs preparation strategy for improving the applicability of BNMs in enhanced bioconversion, drug delivery, and biosensors.

RESULTS AND DISCUSSION

Synthesis and characterization of PNIPAM microgels

The microgels were prepared by precipitation polymerization of NIPAM with BIS cross-linker above their LCST in water in a N_2-filled closed environment (Figure 2A). As the cross-linking agent BIS has higher reactivity than NIPAM, the prepared microgels would show a typical cross-linking gradient from the center toward the outside (Wu et al., 1994). The field emission scanning electron microscopy (FESEM) images of the dried PNIPAM microgels in Figure 2B showed a core-shell structure, with a dense core region of higher cross-linking density and a fuzzy shell that might consist of dangling chains. The diameter of the dried microgels was about 478 nm. The hydrodynamic diameter of PNIPAM microgels at 25°C and 38°C was tested by dynamic light scattering (DLS), which was 675 and 129 nm, respectively, exhibiting superb temperature-responsive volume phase transition

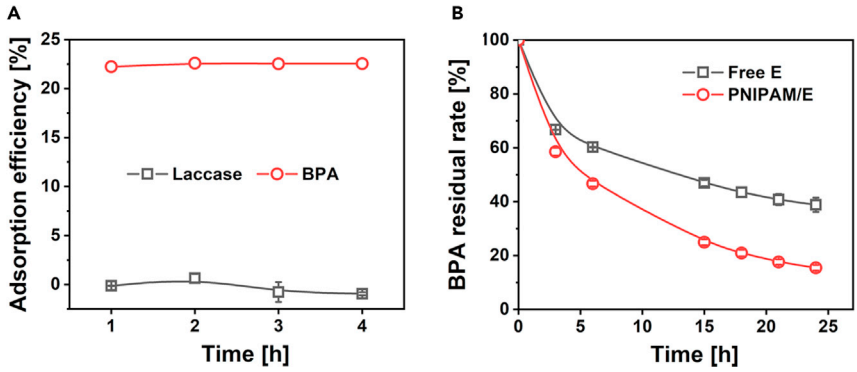

Figure 3. Interactions between PNIPAM microgels, laccase, and BPA

(A) The adsorption capacity of PNIPAM microgels for laccase and BPA, respectively. The concentration of PNIPAM microgels in the experiment was 0.2 mg L^{-1}.

(B) BPA residual rate over reaction time. The concentration of PNIPAM microgels in the experiment was 0.1 mg L^{-1}. The error bars represent the standard deviation of at least three measurements.

characteristics (Figure 2C). They are supposed to play a good gating role in the BNMs. Moreover, the polymer dispersity index values of PNIPAM microgels at 25°C and 38°C were 0.631 and 0.361, respectively, indicating a relatively good dispersibility. The dispersion of the microgels at 38°C was better than that at 25°C. Thereinto, the diameter of PNIPAM microgels at the collapsed status tested by FESEM is larger than that measured by DLS. This is because microgels adsorbed to the solid foil used in FESEM significantly deform under the influence of interfacial tension, which results in the cross sections exceeding their bulk dimensions. Moreover, the surface charge of PNIPAM microgels was −1.44 mV in the acetic acid buffer (pH 5, 10 mM), which was measured by zeta potential analysis.

Interactions between PNIPAM microgels, laccase, and BPA

From the previous studies, the incorporation of nanomaterials with high adsorption ability in the BNM has negative effects on its activity and stability (Zhang et al., 2019b). Thanks to their high hydrophilicity at swollen state, the microgels can inhibit the adsorption of the hydrophobic molecules on its surface (Conzatti et al., 2019). Moreover, their soft and fuzzy surface would produce less flow resistance for solvent and solute molecules, thereby reducing diffusional limitations. However, the swollen microgel is permeable that allows small molecules, such as multivalent ions, proteins, enzymes, and even nanoparticles, to get absorbed into its interior matrix by diffusion. If enzymes were absorbed in its matrix, it would largely increase the internal mass transfer resistance for both substrate and products, leading to low enzyme activity. In this study, the main role of PNIPAM microgels in the BNM is to create a tunable confinement strength to laccase and at the same time endow enzyme with hydrophilic microenvironment. Hence, it is necessary to synthesize the microgels without the absorption ability toward the enzyme. To address this requirement, the PNIPAM microgels with the mesh size smaller than laccase were developed by using a high proportion of cross-linking agent. As shown in Figure 3A, laccase cannot be immobilized on/in microgels. In contrast, BPA can be absorbed and fixed into the microgels network by diffusion owing to its smaller size. The adsorption efficiency reached 22.5% and the adsorption capacity was 9 mg (BPA) g(microgels)$^{-1}$.

After that, we used PNIPAM/laccase (PNIPAM/E) and free laccase (free E) to degrade BPA. The degradation rate of PNIPAM/E was significantly higher than that of free laccase. More than 80% of BPA was degraded by the PNIPAM/E after 24 h, whereas free E could only degrade less than 60% (Figure 3B). It can be attributed to the synergetic effect between PNIPAM adsorption and enzyme catalysis. Therefore, the prepared microgels exhibited desirable traits for further application in the fabrication of the smart BNMs.

PNIPAM-modified NF membrane by *in situ* method at 60°C

Characterization of PNIPAM-modified NF membrane

As seen in Figure 4A, the pristine NF membrane is placed in a home-made cell in reverse mode (support layer facing feed) and a PDA adhesion layer is formed in the inner surface of the support layer by DA

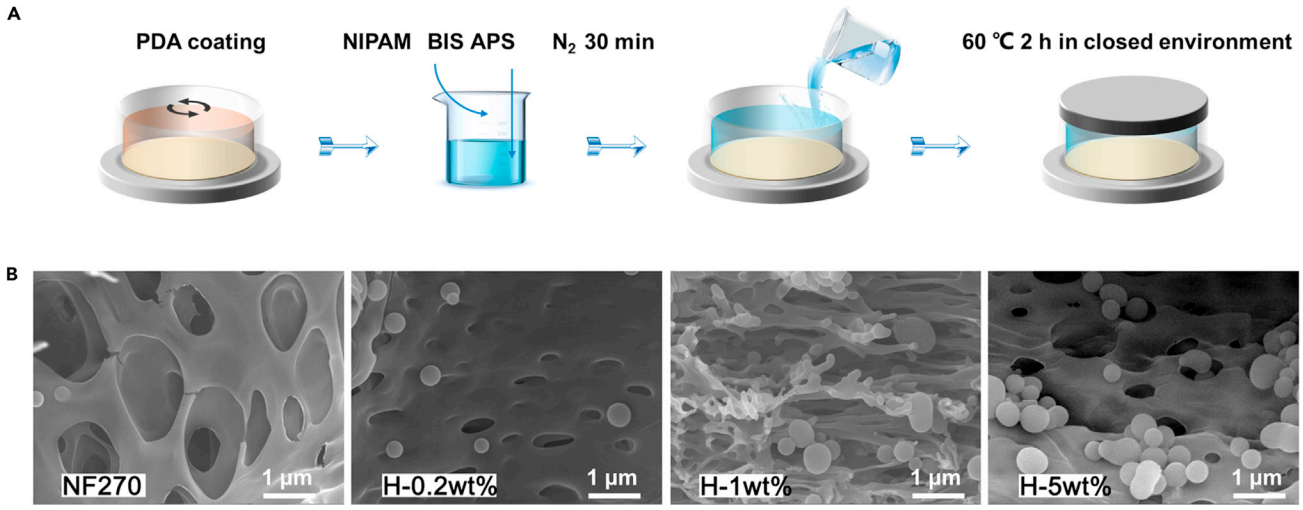

Figure 4. Preparation and characterization of PNIPAM-modified NF membrane by *in situ* method at 60°C

(A) Scheme for modification of the membrane support layer with PNIPAM microgels by *in situ* method at 60°C.

(B) FESEM images of the cross section of NF270, H-0.2wt%, H-1wt%, and H-5wt% membranes.

coating. Subsequently, the deoxygenated monomer solution is added into the cell for *in situ* modification of the membrane at 60°C. Thereinto, the PDA adhesion layer can increase the hydrophilicity of the support layer and thus facilitate its monomer uptake. Moreover, the adhesive property of PDA can stabilize the synthesized PNIPAM microgels in the support layer (Zhang and Serpe, 2015). According to the difference in NIPAM concentration, PNIPAM-modified NF membranes were named as H-0.2wt%, H-1wt%, and H-5wt %. Figure 4B shows FESEM images of the cross-section of the pristine and PNIPAM-modified BNMs. It can be directly seen that the PNIPAM microgels were successfully *in situ* synthesized and confined in the PDA-coated porous support layer of the NF membrane. Furthermore, the number of grafted microgels in the support layer increased with the concentration of the NIPAM monomer used for membrane modification.

Performance of PNIPAM-based BNMs

The BNMs were then fabricated by reversely filtrating laccase into the PNIPAM-modified support layer and termed as H-0.2wt%-E, H-1wt%-E, and H-5wt%-E according to the difference in NIPAM monomer concentration (Figure 5A). In addition, the pristine-E was also prepared by reverse filtration of laccase into the pristine NF270 membrane. Laccase is mainly immobilized by the geometric confinement of the support layer of the NF membrane. Thereinto, PNIPAM modification can enhance the geometric confinement strength and specific surface area of the support layer, which benefits for enzyme immobilization and stabilization (Zhang et al., 2020). Therefore, the enzyme loading of the PNIPAM-modified BNMs was much higher than that of the pristine-E (Figure 5B). Thereinto, enzyme loading increased with the NIPAM monomer concentration used for membrane modification. It was because the higher NIPAM monomer concentration facilitated the formation of more PNIPAM microgels, which further enlarged enzyme immobilization space and reinforced the confinement to laccase (Gao and Frisken, 2003).

Generally, the pore size of the skin layer of the NF membrane determines its permeability. As observed in Figure 5C, the PNIPAM-modified membranes show lower permeability than the pristine membrane, indicating that a part of the microgels or polymer chains conceivably blocked the membrane pores. After enzyme immobilization by reverse filtration, the permeability of the pristine-E dropped sharply, whereas PNIPAM-based BNMs showed a negligible reduction. Hence the permeability of PNIPAM-based BNMs was higher than that of the pristine-E. It can be explained that the PNIPAM modification enhanced compartmentalization and steric effect of the support layer to laccase, which is conductive to broaden enzyme distribution, and prevent enzyme excess migration in the support layer and finally aggregation beneath the skin layer of the NF membrane.

For BPA removal experiments, the BNMs were tested at 25°C in the flow-through mode. In this situation, the microgels were in a swollen state, which would reduce the pore size of the support layer and intensify

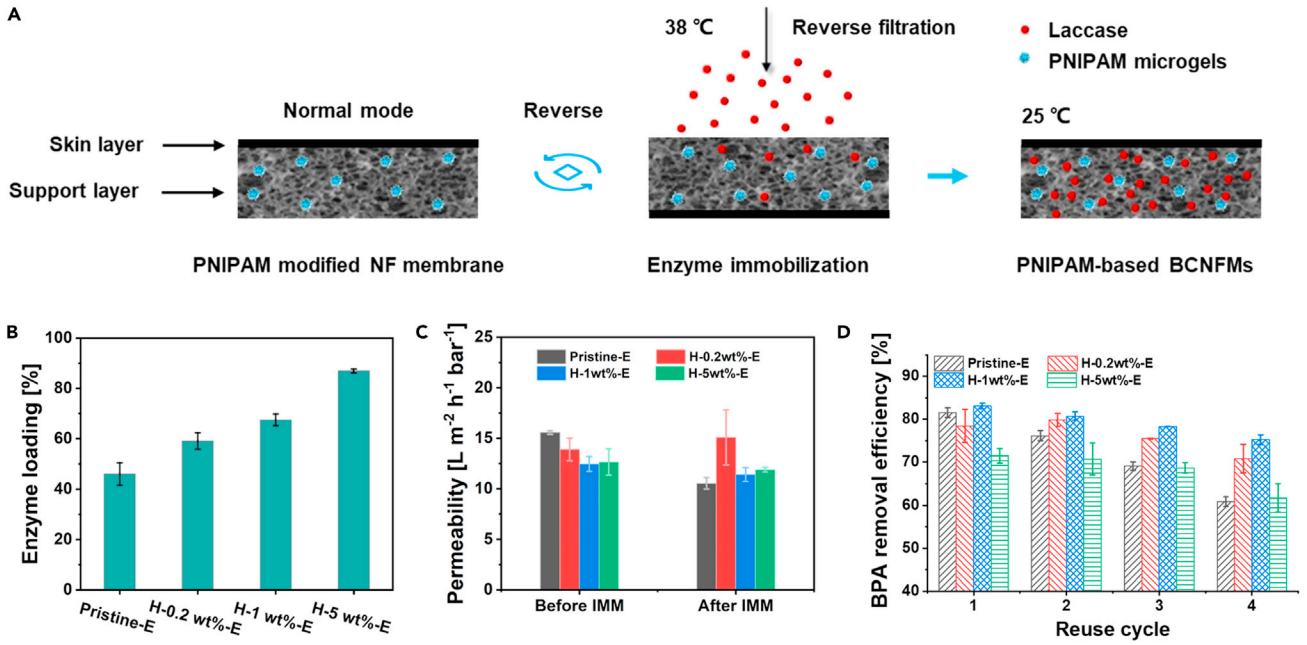

Figure 5. Performance of PNIPAM-based BNMs

(A) Schematic diagram of PNIPAM-based BNMs preparation by "reverse filtration" method.

(B–D) (B) Enzyme loading, (C) membrane permeability variations in different operation stages during preparation, and (D) BPA removal efficiency over four reuse cycles of the pristine-E, H-0.2wt%-E, H-1wt%-E, and H-5wt%-E. IMM refers to immobilization. The error bars represent the standard deviation of at least three measurements.

the geometric confinement to laccase, thereby inhibiting enzyme leakage. As shown in Figure 5D, BPA removal efficiency of these four BNMs in the first cycle was in the order: H-1wt%-E > pristine-E > H-0.2wt%-E > H-5wt%-E. Although enzyme loading in H-5wt%-E was the highest, its BPA removal rate was the lowest. This can be explained by the fact that higher enzyme and microgels loading in the support layer induced higher steric hindrance, which severely hampered the accessibility of the substrate to laccase. Moreover, the high confinement strength of H-5wt%-E to laccase reduced the enzyme mobility and thus suppressed enzyme activity (Zhang et al., 2020). In addition, the PNIPAM-based BNMs showed better operational stability than the pristine-E during four reuse cycles. This was attributed to the enhanced confinement strength of the PNIPAM-based BNMs, thereby reducing enzyme leakage and stabilizing enzyme structure. Thereinto, H-1wt%-E exhibited the highest BPA removal efficiency (83.08% in the first reuse cycle) and the best reusability (average decline of each cycle is only 1.96%), meaning that laccase in H-1wt%-E had the most suitable confinement strength, enzyme loading, and immobilization microenvironment.

Analysis of BPA removal efficiency decline during reuse

However, with the increase of reuse cycles, the BPA removal efficiency of the PNIPAM-based BNMs was still decreased (Figure 5D). This may be caused by the combination of multiple reasons including enzyme leakage, products accumulation, and enzyme conformation change. Thereinto, the products accumulation and enzyme leakage problems in these three PNIPAM-based BNMs were discussed in the following part.

The literature suggests that, during the reaction between BPA and laccase, low-molecular-weight (LMW) products such as phenol and 4-isopropenylphenol are first formed. Then high-molecular-weight (HMW) polymers are formed by further condensation reaction of intermediate products (Catherine et al., 2016; Galliker et al., 2010). In our studies, by means of HPLC analysis, two peaks with shorter retention time than the BPA peak were identified in BPA degradation permeate, indicating LMW products were produced after the treatment of BPA by BNMs (Figure 6A). We named these two LMW products as product (I) and (II). As shown in Figure 6B, the ratio of LMW product (I) to the degradation products in the permeate decreased with the increase of reuse cycles, indicating it might accumulate in the membrane or be further converted to HMW products. Those HMW products are more likely to accumulate in the membrane. Such product accumulation phenomenon was detrimental to the activity and stability of the immobilized laccase. Among

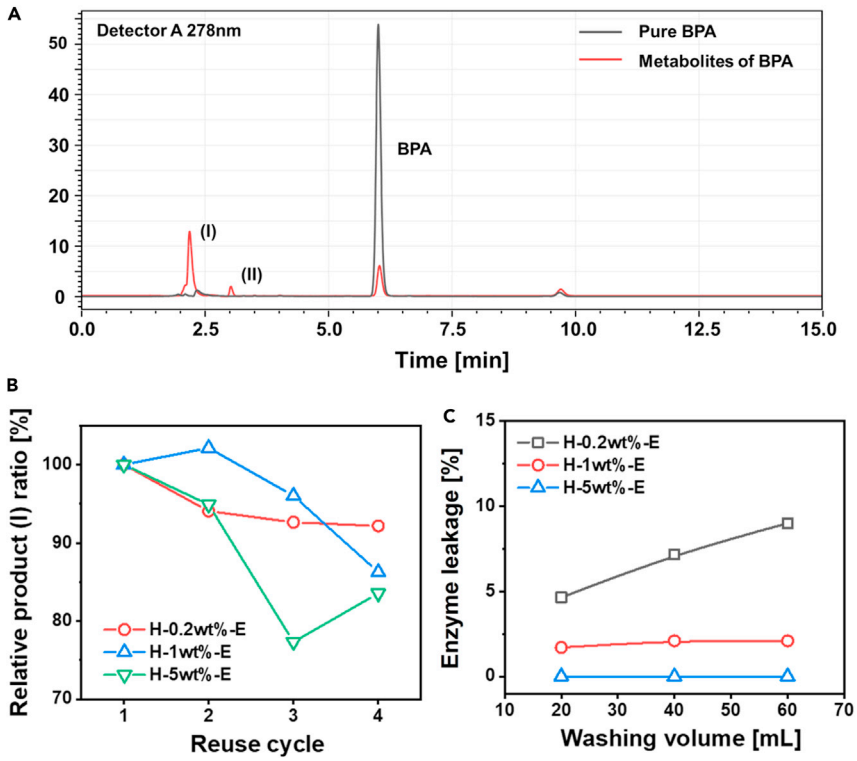

Figure 6. Analysis of BPA removal efficiency decline during reuse

(A) HPLC spectra of BPA solution and degraded sample solution.

(B) The ratio of products (I) to the degradation products in the permeate.

(C) Enzyme leakage of H-0.2wt%-E, H-1wt%-E, and H-5wt%-E during washing under flow-through mode.

these three BNMs, H-5wt%-E showed the highest decline degree of product (I), revealing the most serious products accumulation due to its strongest confinement strength. After three reuse cycles, the proportion of product (I) in the permeate of H-5wt%-E increased because of product adsorption saturation and the excess product (I) leaking out.

As shown in Figure 6C, H-1wt%-E and H-5wt%-E exhibited negligible enzyme leakage after being washed with 60 mL acetic acid buffer at 25°C owing to their high confinement strength. The enzyme leakage in H-0.2wt%-E reached 9%. Therefore, for H-0.2wt%-E, the decline in BPA removal was caused by both enzyme leakage and products accumulation, whereas for H-1wt%-E and H-5wt%-E, the BPA removal decline was mainly caused by products accumulation.

Regeneration

When the immobilized enzyme is partly deactivated, the BNMs need to be regenerated by elution-cleaning-reloading processes. According to our previous assumptions, when the operating temperature is higher than the LCST of PNIPAM (32°C), the microgels would be in a collapsed state, which endows the support layer with a relatively large pore size and thus reduces its geometric confinement to laccase. In this situation, laccase can be easily eluted. Unexpectedly, as seen in Figure 7A, when we eluted the immobilized laccase at 38°C (T > LCST), the H-0.2wt%-E showed the highest protein elution rate, which was only 47%, whereas that of the other two PNIPAM-based BNMs was even lower than 20%, which is far below our expectation.

The microgels in the support layer are in a collapsed state when *in situ* synthesized at 60°C. Therefore, we speculate that excess growth of microgels in the membrane occurred (Figure 7B). Consequently, the confinement strength of the support layer to laccase is still very high even at 38°C (T > LCST), making laccase still difficult to be eluted. Therefore, *in situ* synthesis of PNIPAM microgels in the membrane at 25°C (T < LCST) was evaluated in the next section. It is speculated that the microgels are in a swollen state during the synthesis process at 25°C, which may inhibit their growth in the support layer and avoid excess filling in

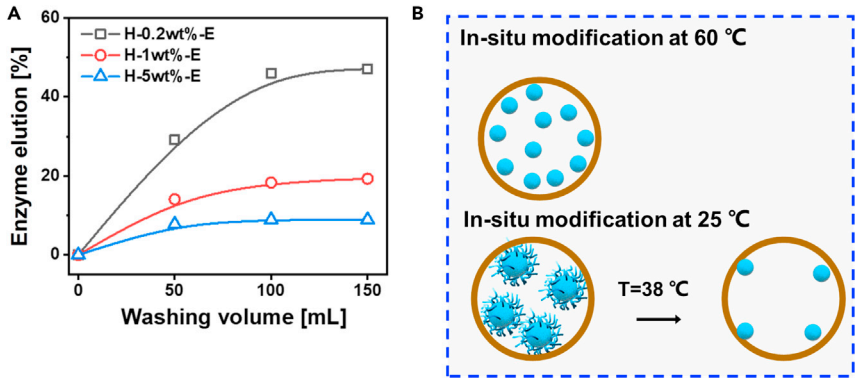

Figure 7. Regeneration of PNIPAM-based BNMs

(A) Enzyme elution of NF270, H-0.2wt%-E, H-1wt%-E, and H-5wt%-E.

(B) Schematic diagram for the difference of *in situ* microgels growth in support layer at 25°C and 38°C.

the pores. Furthermore, when operated at high temperature, the microgels docked in the support layer are supposed to switch to a collapsed state, which opens the pores of the support layer and facilitates enzyme elution from the membrane (Figure 7B).

PNIPAM-modified NF membrane by *in situ* method at 25°C

APS and TEMED were used as co-initiators to *in situ* synthesize PNIPAM microgels in the PDA-modified support layer of the NF membrane at 25°C, and the number of grafted microgels was controlled by the reaction time (Figure 8A). The successful modification of the support layer by PNIPAM microgels at 25°C can be confirmed by the FESEM images shown in Figure 8B. Unexpectedly, the number of the grafted microgels in the support layer at 25°C seemed larger than that synthesized at 60°C. This may be attributed to the high react activity of the newly added TEMED initiator. Moreover, the number of the grafted microgels increased with modification time. In addition, the hydrophilicity of the PNIPAM-modified support layer was significantly enhanced compared with the pristine one (Figure 8C). According to the zeta potential analysis, the PNIPAM-modified support layer showed a negative charge at pH 5 (Figure 8D), implying that the following immobilization of laccase (negatively charged at pH 5) was mainly caused by geometric confinement (no electrostatic attraction).

Contrary to the previous result in Figure 5B, it is surprising that the enzyme loading decreased with increase in the number of grafted microgels (Figure 9A). This was because a plenty of grafted microgels severely blocks the pores of the support layer, impeding the laccase access into the membrane during reverse filtration. In addition, the synthesized microgels were in a swollen state, making it hard to get close to the skin layer. Therefore, the permeability of the NF membrane after PNIPAM modification exhibited little decline compared with the pristine one (Figure 9B). Moreover, the permeability decline of the PNIPAM-based BNMs was much lower than that of the pristine-E after enzyme loading owing to the enhanced compartmentalization and steric effect caused by PNIPAM *in situ* modification at 25°C.

According to the difference in modification time, the BNMs prepared by *in situ* modification at room temperature (25°C) were termed as R-0.5h-E, R-1h-E, and R-2h-E. As shown in Figure 9C, the BPA removal efficiency of these four BNMs in the first cycle was in the order: R-2h-E > pristine-E > R-1h-E > R-0.5h-E. Although the enzyme loading in R-0.5h-E was the highest and the grafting number of microgels was the lowest, its BPA removal efficiency was still the lowest. This result indicated that crowded enzymes in a confined space cannot fully exert their activity due to the high mass transfer resistance. In addition, the PNIPAM-based BNMs prepared by *in situ* method at 25°C also showed better reusability than the pristine-E. Because of their high steric hindrance, such PNIPAM-based BNMs showed severe products accumulation problems and no enzyme leakage (Figures 9D and 9E). Thereinto, the R-0.5h-E showed the worst stability during four reuse cycles owing to its most serious products accumulation. The R-2h-E exhibited the highest BPA removal efficiency (82.5% in the first reuse cycle) and the best stability during four reuse cycles (the average decline of each cycle is only 3.02%). In the regeneration experiments, the highest protein elution rate was only 17.9%, which was still lower than our expectation. Therefore, in situ modification could effectively increase the geometric confinement of

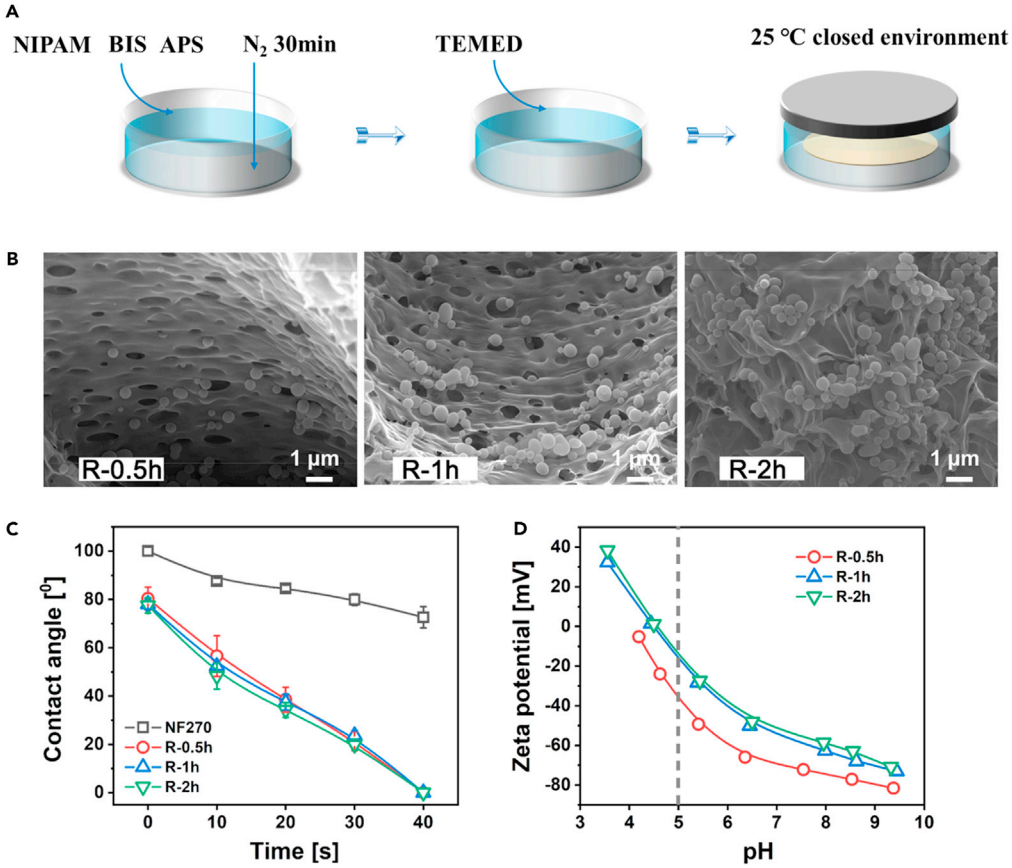

Figure 8. Preparation and Characterization of PNIPAM-modified NF membrane by *in situ* method at 25°C

(A) Scheme for modification of the membrane support layer with PNIPAM microgels by *in situ* method at 25°C.

(B) FESEM images of the cross section of R-0.5h, R-1h, and R-2h membranes.

(C and D) (C) contact angle and (D) zeta potential of the support layer of R-0.5h-E, R-1h-E, and R-2h-E membranes. The error bars represent the standard deviation of at least three measurements.

the support to laccase and create a hydrophilic microenvironment that ameliorated the reusability of the BNMs. However, the PNIPAM microgels are hydrophobic when operated at 38°C (T > LCST), which would impede enzyme elution due to hydrophobic adsorption (Xiao et al., 2013). Moreover, the *in situ* modification process is difficult to control, and besides microgels, there may exist immature PNIPAM microgels with smaller sizes being docked in the support layer, which makes the fabricated PNIPAM-based BNMs fail to achieve the purpose of enzyme elution-reloading and performance regeneration.

PNIPAM-PEI-based BNMs

From the above analysis, microgels armed with durable hydrophilicity are preferred. Furthermore, to make the modification process more controllable, we propose to use the pre-synthesized PNIPAM-PEI microgels to modify the membrane by co-deposition method. PNIPAM-PEI microgels are synthesized via graft copolymerization of NIPAM and BIS from PEI in the presence of initiator t-BuOOH (Figure 10A). The synthesized PNIPAM-PEI microgels have the PNIPAM core and hydrophilic PEI shell, which would endow them with durable hydrophilicity even in a collapsed state (Dubey et al., 2015; Leung et al., 2004). As seen in Figure 10B, the FESEM images of the dried PNIPAM-PEI microgels showed a core-shell structure. The diameter of the dried PNIPAM-PEI microgels was about 250 nm. The hydrodynamic diameter of PNIPAM-PEI microgels at 25°C and 38°C was tested by DLS, which was 440 and 293 nm, respectively, exhibiting admirable temperature-responsive property (Figure 10C). Moreover, since PNIPAM-PEI microgels have a positive surface charge of 2.17 mV (due to the grafting of the cationic PEI chains) and the surface charge of laccase is −4.6 mV at pH 5 (Zhang et al., 2020), laccase would be immobilized by electrostatic adsorption besides geometric confinement.

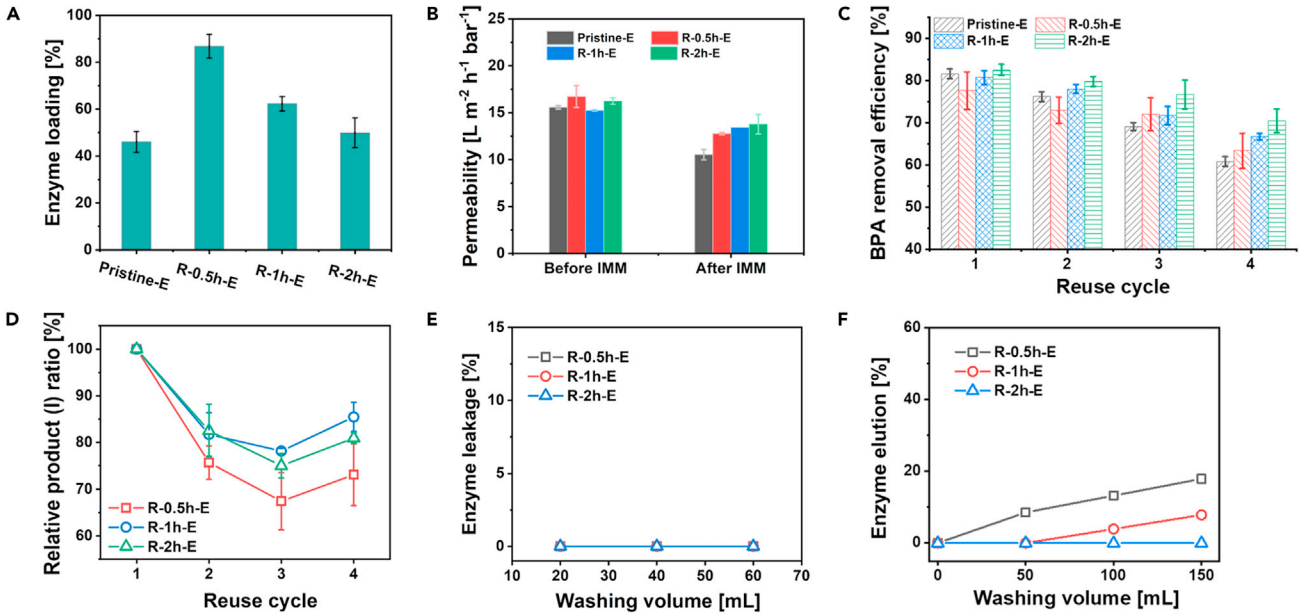

Figure 9. Performance of PNIPAM-based BNMs

(A) Enzyme loading, (B) membrane permeability, (C) BPA removal efficiency, (D) the ratio of products (I) to the degradation products in the permeate, (E) enzyme leakage, and (F) enzyme elution efficiency of pristine-E, R-0.5h-E, R-1h-E, and R-2h-E membranes. IMM refers to immobilization. The error bars represent the standard deviation of at least three measurements.

Figure 11A showed the scheme for the modification of the support layer by PDA/PNIPAM-PEI co-deposition method. PNIPAM-PEI-modified membranes were termed as PEI-1h-E, PEI-2h-E, and PEI-4h-E according to the difference in modification time. As observed in Figure 11B, microgels were successfully immobilized in the support layer. Moreover, unlike NF270, the support layer of PEI-2h was positively charged after co-deposition modification, further confirming that laccase can be also immobilized by electrostatic adsorption (Figure 11C). Compared with the *in situ* modification method, the PNIPAM-PEI microgels would be more stable

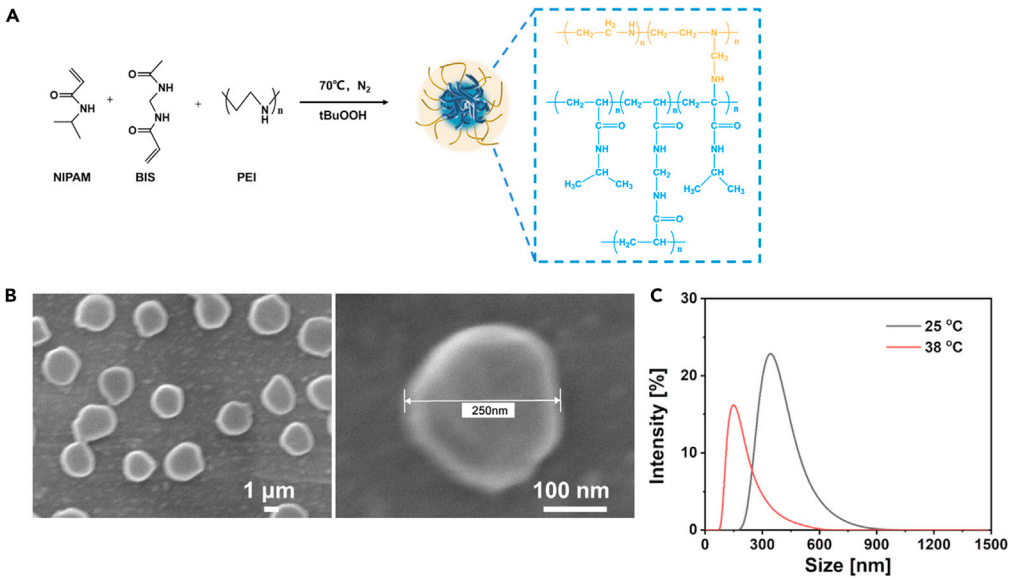

Figure 10. Synthesis and characterization of PNIPAM-PEI microgels

(A) Scheme for the synthesis of PNIPAM-PEI microgels.

(B) FESEM images of PNIPAM.

(C) DLS measurement of the size distribution of PNIPAM-PEI microgels under 25°C and 38°C, respectively.

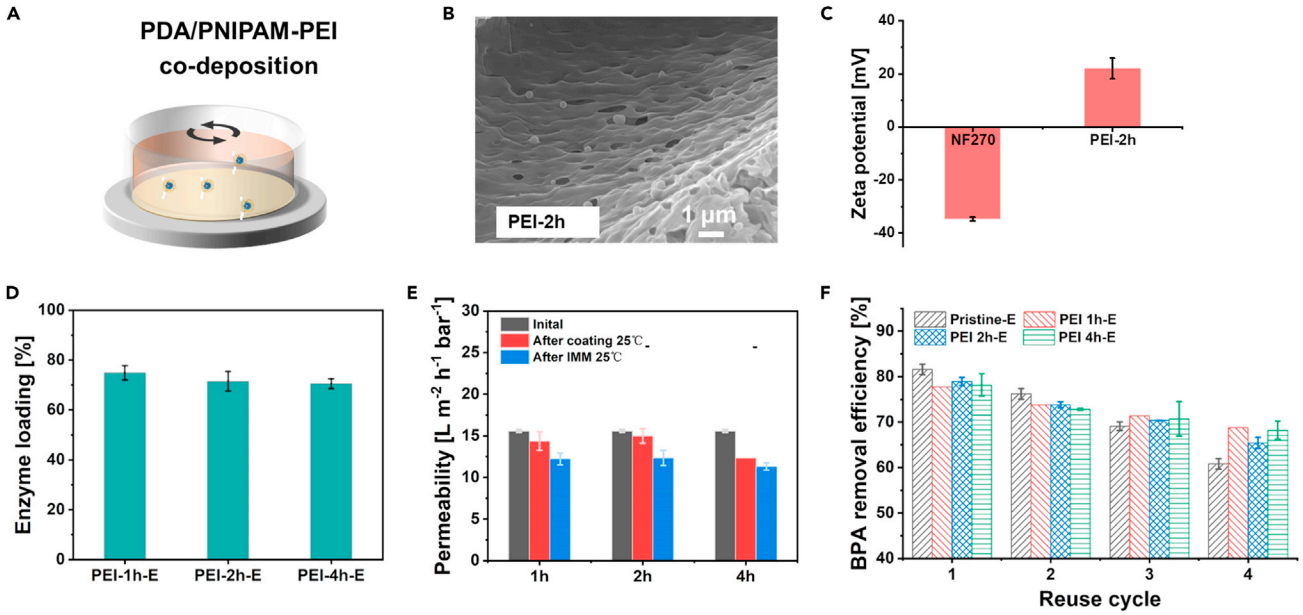

Figure 11. Characterization and the performance of PNIPAM-PEI-based BNMs

(A) Scheme for the modification of the support layer by the PDA/PNIPAM-PEI co-deposition method.

(B) FESEM image of the cross section of PEI-2h.

(C) Zeta potential of the support layer of NF270 and PEI-2h membranes.

(D–F) (D) Enzyme loading, (E) permeability variations in different operation stages during preparation (F), and BPA removal efficiency of PEI-1h-E, PEI-2h-E, and PEI-4h-E. The error bars represent the standard deviation of at least three measurements.

as it is immobilized by the covalent bond between PEI and PDA coating layer. The enzyme loading of PEI-1h-E, PEI-2h-E, and PEI-4h-E was almost the same, which was above 70% (Figure 11D). The permeability decreased after co-deposition modification and enzyme immobilization due to pore blocking (Figure 11E). Thereinto, the enzyme loading of the pristine-E was the lowest, but its BPA removal efficiency in the first reuse cycle was higher than that of the PNIPAM-PEI-based BNMs (Figure 11F). This was because the high confinement strength of PNIPEM-PEI-based BNMs largely constricted the essential mobility of the immobilized laccase for efficient catalysis and thus led to a lower BPA removal efficiency (Zhang et al., 2020). In contrast, the low enzyme mobility in PNIPEM-PEI-based BNMs significantly delayed the enzyme leakage, resulting in better reusability (Figure 11F). In addition, the BPA removal efficiency and reusability of PEI-1h-E, PEI-2h-E, and PEI 4h-E are almost the same.

In the enzyme elution process, PEI-2h-E was successively washed with deionized water at 25°C (60 mL), deionized water at 38°C (60 mL), and NaOH solution at 38°C (pH 10, 60 mL). It can be seen that few enzymes were eluted and the permeability of the membrane did not change when washing with deionized water at 25°C (Figures 12A and 12B). When washing with deionized water at 38°C, the protein elution rate dramatically increased. The permeability of the membrane also increased. Finally, the protein elution rate exceeded 80% after NaOH washing as NaOH could inhibit the electrostatic adsorption of laccase. Therefore, we performed the above-mentioned protein elution operation for PEI-2h-E after four reuse cycles and subsequently soaked it in deionized water shaking at 120 rpm for 2 h. After that, the fresh laccase was reloaded in the PEI-2h membrane. As shown in Figure 12C, the enzyme loading was the same as that for the first BNM preparation. Moreover, the BPA removal performance of the regenerated PEI-2h-E (5–8 cycles) was comparable with that in the first four cycles, confirming that the PNIPAM-PEI-based BNMs can achieve rapid regeneration (Figure 12D). Such regeneration ability of our BNMs could benefit the sustainable use of the BNMs thereby facilitating their practical application. Moreover, compared with other laccase-based BNMs reported in the recent literature, the PNIPAM- and PNIPAM-PEI-based BNMs exhibited great advantages in BPA removal efficiency and operation stability (Table 1).

Mechanism discussion

The support layer of the pristine membrane NF270 has a hierarchical porous structure with a gradient pore size (Figure S1). For the *in situ* modification method, some immature PNIPAM microgels may *in situ* grow in

Table 1. Comparison of the laccase-based biocatalytic membranes for BPA removal

Biocatalytic membranes	Initial BPA concentration (mg L^{-1})	Feed volume (mL)	Operation time every cycle (h)	BPA removal efficiency in the first cycle (mg (BPA)/h×10^{-3})	Reuse cycle	BPA removal efficiency in the last cycle (mg (BPA)/h×10^{-3})	Throughput (L m^{-2} h^{-1})	Average decline per cycle (%)	Regeneration ability	Reference
TiO_2 (sol-gel)-PVDF (MF)	34.24	40	24	52.5	4	47.9	1.98	2.00	No	(Hou et al., 2014)
Cu-IDA-PEI-PVDF (MF)	10	8.8	6	14.5	5	8.4	10	8.40	Good	(Fan et al., 2017)
PAN-MIL-101 (UF)	10	40	5	73.6	7	49.6	6.45	4.29	No	(Ren et al., 2018)
PDA-NF270	10	40	5	70.4	7	27.20	5.97	7.70	No	(Cao et al., 2016)
Cu-PDA-NF270	2	20	6	5.80	9	5.1	2.49	1.11	No	(Cao et al., 2018)
GO/PDA-NF270	10	30	3	67	4	37	7.46	7.50	No	(Zhang et al., 2019a)
PEI-E	10	30	3	80	7	77	7.46	0.43	No	(Zhang et al., 2020)
Pristine-E	10	15	1.5	81.58	4	60.80	7.46	5.20	Poor	
H-1wt%-E	10	15	1.5	83.08	4	75.26	7.46	1.96	Poor	This work
R-2h-E	10	15	1.5	82.50	4	70.47	7.46	3.00	Poor	This work
PEI 2h-E	10	15	1.5	78.95	4	68.20	7.46	2.69	Good	This work

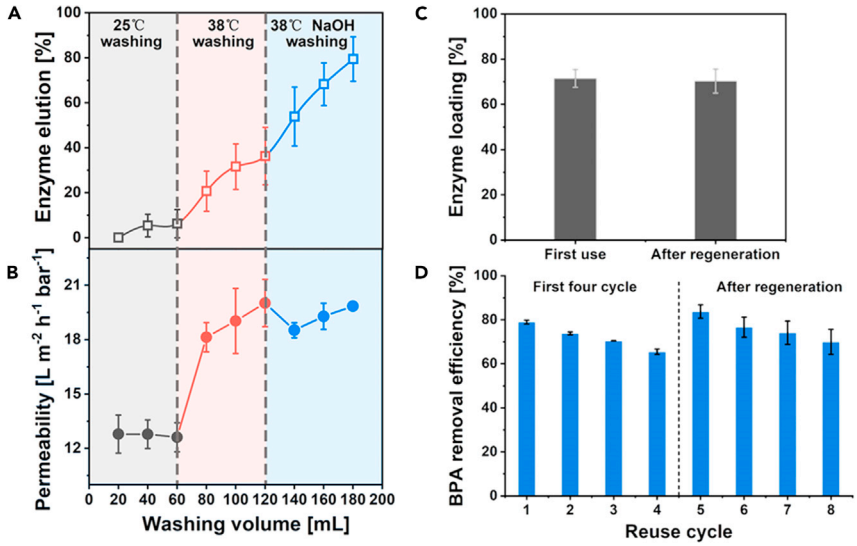

Figure 12. Regeneration of PNIPAM-PEI-modified BNM

(A and B) (A) Enzyme elution efficiency and (B) permeability variations of PEI 2h-E.

(C) Enzyme loading of firstborn and regenerated PEI 2h-E.

(D) BPA removal efficiency of PEI 2h-E during the first reuse cycles (1–4 cycle) and another four reuse cycles (5–8 cycle) after regeneration (operated at 25°C). The error bars represent the standard deviation of at least three measurements.

the small pores of the support layer, which further enhances the compartmentalization and geometric effect of the support layer, thus preventing the flux decline caused by enzyme aggregation beneath the skin layer (Figures 5B, 9B, and 13). However, it also increases the difficulties for enzyme elution (Figures 7A and 9F). The co-deposition of PDA/PNIPAM-PEI cannot insert the PNIPAM-PEI microgels into the pores with the size smaller than microgels, which makes the enzyme elution process easier (Figures 12A, 13, and S2). However, a part of laccase would go through the microgels area and stack beneath the skin layer, leading to a higher reduction in membrane permeability and lower catalytic efficiency compared with PNIPAM-based BNMs (Figure 11, Table 1).

CONCLUSION

In this study, the temperature-responsive PNIPAM-based BNMs with nanogating function were successfully fabricated for the first time. PNIPAM modification enhanced the geometric confinement strength of the support layer, which effectively improved enzyme loading, reduced enzyme leakage, and prohibited membrane permeability reduction caused by the aggregation of laccase in the membrane. Moreover, the flexible and reversible adjustment of pore sizes of the porous support layer was achieved by the "swelling/collapse" switch of microgels, thus realizing large-extent self-regulation of the confinement strength of the NF membrane to laccase. Benefiting from this feature, the PNIPAM-based BNMs exhibited good performance in different operation scenarios. When applied for BPA removal, the PNIPAM-based BNMs were operated at 25°C (T < LCST). The microgels were in a swollen state, which offered a high confinement strength and hydrophilic microenvironment to immobilized laccase and thus stabilized enzyme structure and prevented enzyme leakage. By optimizing the concentration of reaction monomers, modification time, and methods, the prepared PNIPAM-based BNM showed high BPA removal efficiency and stability, which was superior to most results in the literature. In addition, the PNIPAM-PEI-based BNMs can be easily regenerated through the elution-washing-reloading process when operated at 38°C (T > LCST, microgels were in a collapsed state, which led to a low confinement strength to laccase), and the laccase activity and BPA removal efficiency were fully recovered. This work provides a new design strategy to fabricate BNM with high catalytic efficiency, long-term stability, and good regeneration properties, which may facilitate the potential applications of BNMs in bioconversion, drug delivery, and biosensors.

Limitations of the study

Based on the results, we speculate that there exist immature microgels in the small pores of the support layer by *in situ* modification process, but they are not found in FESEM images. Advanced characterization

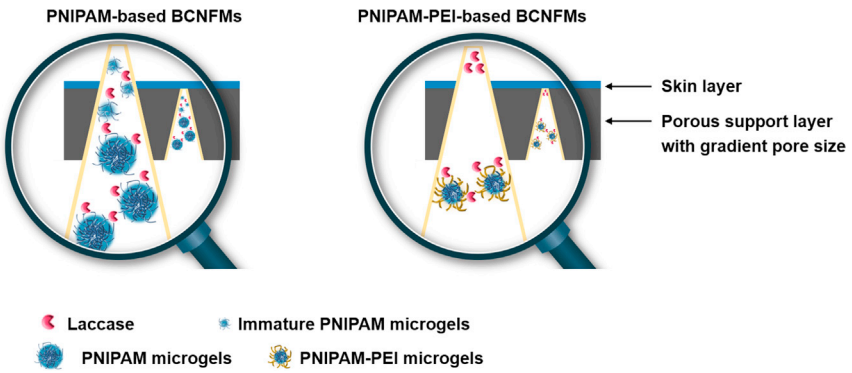

Figure 13. Potential mechanism of enzyme immobilization and elution process in PNIPAM-based and PNIPAM-PEI-based BNMs.

techniques (e.g., *in situ* detection of enzyme after immobilization and immature microgels) are urgently needed to visualize the exact distribution of all components in the membrane, which would facilitate the precise design of the enzyme immobilization process. Advanced characterization techniques are urgently needed to visualize the exact distribution of all components in the membrane, which would exercise a crucial influence on the precise design of the enzyme immobilization process. Furthermore, the stability of the BNMs for treating the real contaminated water is still to be explored. Lastly, although we analyzed the BPA degradation products by HPLC, further analysis of the products evolution and molecular composition is also needed.

STAR★METHODS

Detailed methods are provided in the online version of this paper and include the following:

- KEY RESOURCES TABLE
- RESOURCE AVAILABILITY
  - Lead contact
  - Materials availability
  - Data and code availability
- METHOD DETAILS
  - Microgel synthesis and characterization
  - Preparation and characterization of PNIPAM modified membrane
  - Preparation and characterization of biocatalytic nanofiltration membranes (BNMs)
  - Mechanism analysis of BPA removal efficiency decline during reuse
  - Regeneration of the BNM

SUPPLEMENTAL INFORMATION

Supplemental information can be found online at https://doi.org/10.1016/j.isci.2021.103671.

ACKNOWLEDGMENTS

This work was supported by the National Natural Science Foundation of China (No. 21878306) and the Beijing Natural Science Foundation (2192053).

AUTHOR CONTRIBUTIONS

Conceptualization, methodology, and investigation, H.Z. and J.Q.L.; writing - original draft, H.Z.; writing - review & editing, H.Z. and J.Q.L.; supervision, J.Q.L. and Y.H.W.

DECLARATION OF INTERESTS

The authors declare no competing interests.

Received: August 26, 2021
Revised: November 18, 2021
Accepted: December 14, 2021
Published: January 21, 2022

REFERENCES

Barbhuiya, N.H., Misra, U., and Singh, S.P. (2022). Biocatalytic membranes for combating the challenges of membrane fouling and micropollutants in water purification: a review. Chemosphere *286*, 131757.

Cao, X., Luo, J., Woodley, J.M., and Wan, Y. (2016). Bioinspired multifunctional membrane for aquatic micropollutants removal. ACS Appl. Mater. Inter. *8*, 30511–30522.

Cao, X., Luo, J., Woodley, J.M., and Wan, Y. (2018). Mussel-inspired co-deposition to enhance bisphenol A removal in a bifacial enzymatic membrane reactor. Chem. Eng. J. *336*, 315–324.

Catherine, H., Penninckx, M., and Frédéric, D. (2016). Product formation from phenolic compounds removal by laccases: a review. Environ. Technol. Inno. *5*, 250–266.

Cen, Y.K., Liu, Y.X., Xue, Y.P., and Zheng, Y.G. (2019). Immobilization of enzymes in/on membranes and their applications. Adv. Synth. Catal. *361*, 5500–5515.

Conzatti, G., Ayadi, F., Cavalie, S., Carrère, N., and Tourrette, A. (2019). Thermosensitive PNIPAM grafted alginate/chitosan PEC. Appl. Sur. Sci. *467-468*, 940–948.

Daronch, N.A., Kelbert, M., Pereira, C.S., de Araújo, P.H.H., and de Oliveira, D. (2020). Elucidating the choice for a precise matrix for laccase immobilization: a review. Chem. Eng. J. *397*, 125506.

Dubey, N.C., Tripathi, B.P., Muller, M., Stamm, M., and Ionov, L. (2015). Enhanced activity of acetyl CoA synthetase adsorbed on smart microgel: an implication for precursor biosynthesis. ACS Appl. Mater. Inter. *7*, 1500–1507.

Fan, J., Luo, J., and Wan, Y. (2017). Aquatic micro-pollutants removal with a biocatalytic membrane prepared by metal chelating affinity membrane chromatography. Chem. Eng. J. *327*, 1011–1020.

Galliker, P., Hommes, G., Schlosser, D., Corvini, P.F.X., and Shahgaldian, P. (2010). Laccase-modified silica nanoparticles efficiently catalyze the transformation of phenolic compounds. J. Colloid Interf. Sci. *349*, 98–105.

Gao, J., and Frisken, B.J. (2003). Influence of reaction conditions on the synthesis of self-cross-linked N-isopropylacrylamide microgels. Langmuir *19*, 5217–5222.

Grandclement, C., Seyssiecq, I., Piram, A., Wongwahchung, P., Vanot, G., Tiliacos, N., Roche, N., and Doumenq, P. (2017). From the conventional biological wastewater treatment to hybrid processes, the evaluation of organic micropollutant removal: a review. Water Res. *111*, 297–317.

Hou, J., Dong, G., Ye, Y., and Chen, V. (2014). Enzymatic degradation of bisphenol-A with immobilized laccase on TiO2 sol–gel coated PVDF membrane. J. Membr. Sci. *469*, 19–30.

Jochems, P., Satyawali, Y., Diels, L., and Dejonghe, W. (2011). Enzyme immobilization on/in polymeric membranes: status, challenges and perspectives in biocatalytic membrane reactors (BMRs). Green. Chem. *13*, 1609.

Leung, M.F., Zhu, J., Harris, F.W., and Li, P. (2004). New route to smart core-shell polymeric microgels: synthesis and properties. Macromol. Rapid Commun. *25*, 1819–1823.

Li, X., Xu, Y., Goh, K., Chong, T.H., and Wang, R. (2020). Layer-by-layer assembly based low pressure biocatalytic nanofiltration membranes for micropollutants removal. J. Membr. Sci. *615*, 118514.

Liu, J., Yu, L.J., Yue, G., Wang, N., Cui, Z., Hou, L., Li, J., Li, Q., Karton, A., and Cheng, Q. (2019a). Thermoresponsive graphene membranes with reversible gating regularity for smart fluid control. Adv. Funct. Mater. *29*, 1808501.

Liu, Y.-l., Wang, X.-m., Yang, H.-w., Xie, Y.F., and Huang, X. (2019b). Preparation of nanofiltration membranes for high rejection of organic micropollutants and low rejection of divalent cations. J. Membr. Sci. *572*, 152–160.

Liu, Z., Wang, W., Xie, R., Ju, X.J., and Chu, L.Y. (2016). Stimuli-responsive smart gating membranes. Chem. Soc. Rev. *45*, 460–475.

Luo, J., Song, S., Zhang, H., Zhang, H., Zhang, J., and Wan, Y. (2020). Biocatalytic membrane: go far beyond enzyme immobilization. Eng. Life Sci. *19*, 749–758.

Ma, X.Y., Li, Q., Wang, X.C., Wang, Y., Wang, D., and Ngo, H.H. (2018). Micropollutants removal and health risk reduction in a water reclamation and ecological reuse system. Water Res. *138*, 272–281.

Mazzei, R., Yihdego Gebreyohannes, A., Papaioannou, E., Nunes, S.P., Vankelecom, I.F.J., and Giorno, L. (2021). Enzyme catalysis coupled with artificial membranes towards process intensification in biorefinery- a review. Bioresour. Technol. *335*, 125248.

Nöth, M., Gau, E., Jung, F., Davari, M.D., El-Awaad, I., Pich, A., and Schwaneberg, U. (2020). Biocatalytic microgels (μ-Gelzymes): synthesis, concepts, and emerging applications. Green. Chem. *22*, 8183–8209.

Plamper, F.A., and Richtering, W. (2017). Functional microgels and microgel systems. Acc. Chem. Res. *50*, 131–140.

Popat, A., Hartono, S.B., Stahr, F., Liu, J., Qiao, S.Z., and Lu, G.Q. (2011). Mesoporous silica nanoparticles for bioadsorption, enzyme immobilisation, and delivery carriers. Nanoscale *3*, 2801–2818.

Qiao, J., Jiang, J., Liu, L., Shen, J., and Qi, L. (2019). Enzyme reactor based on reversible pH-controlled catalytic polymer porous membrane. ACS Appl. Mater. Inter. *11*, 15133–15140.

Reinicke, S., Fischer, T., Bramski, J., Pietruszka, J., and Böker, A. (2019). Biocatalytically active microgels by precipitation polymerization of N-isopropyl acrylamide in the presence of an enzyme. RSC Adv. *9*, 28377–28386.

Ren, Z., Luo, J., and Wan, Y. (2018). Highly permeable biocatalytic membrane prepared by 3D modification: metal-organic frameworks ameliorate its stability for micropollutants removal. Chem. Eng. J. *348*, 389–398.

Rey, M., Fernandez-Rodriguez, M.A., Karg, M., Isa, L., and Vogel, N. (2020). Poly-N-isopropylacrylamide nanogels and microgels at fluid interfaces. Acc. Chem. Res. *53*, 414–424.

Roman, M., Roman, P., Verbeke, R., Gutierrez, L., Vanoppen, M., Dickmann, M., Egger, W., Vankelecom, I., Post, J., Cornelissen, E., et al. (2021). Non-steady diffusion and adsorption of organic micropollutants in ion-exchange membranes: effect of the membrane thickness. iScience *24*, 102095.

Saad, A., Mills, R., Wan, H., Mottaleb, M.A., Ormsbee, L., and Bhattacharyya, D. (2020). Thermo-responsive adsorption-desorption of perfluoroorganics from water using PNIPAm hydrogels and pore functionalized membranes. J. Membr. Sci. *599*, 117821.

Sha, F., Chen, Y., Drout, R.J., Idrees, K.B., Zhang, X., and Farha, O.K. (2021). Stabilization of an enzyme cytochrome c in a metal-organic framework against denaturing organic solvents. iScience *24*, 102641.

Varga, B., Somogyi, V., Meiczinger, M., Kováts, N., and Domokos, E. (2019). Enzymatic treatment and subsequent toxicity of organic micropollutants using oxidoreductases - a review. J. Clean. Prod. *221*, 306–322.

Vitola, G., Buning, D., Schumacher, J., Mazzei, R., Giorno, L., and Ulbricht, M. (2017). Development of a novel immobilization method by using microgels to Keep enzyme in hydrated microenvironment in porous hydrophobic membranes. Macromol. Biosci. *17*, 1600381.

Wu, X.Y., Pelton, R.H., Hamielec, A.E., Woods, D.R., and Mcphee, W. (1994). The kinetics of poly(N-isopropylacrylamide) microgel latex formation. Colloid Polym. Sci. *272*, 467–477.

Xiao, L., Isner, A.B., Hilt, J.Z., and Bhattacharyya, D. (2013). Temperature responsive hydrogel with reactive nanoparticles. J. Appl. Polym. Sci. *128*, 1804–1814.

Yoon, Y., Westerhoff, P., Snyder, S.A., and Wert, E.C. (2006). Nanofiltration and ultrafiltration of

endocrine disrupting compounds, pharmaceuticals and personal care products. J. Membr. Sci. *270*, 88–100.

Zdarta, J., Meyer, A.S., Jesionowski, T., and Pinelo, M. (2019). Multi-faceted strategy based on enzyme immobilization with reactant adsorption and membrane technology for biocatalytic removal of pollutants: a critical review. Biotechnol. Adv. *37*, 107401.

Zhang, H., Luo, J., Li, S., Woodley, J.M., and Wan, Y. (2019a). Can graphene oxide improve the performance of biocatalytic membrane? Chem. Eng. J. *359*, 982–993.

Zhang, H., Luo, J., Woodley, J.M., and Wan, Y. (2020). Confining the motion of enzymes in nanofiltration membrane for efficient and stable removal of micropollutants. Chem. Eng. J. *421*, 127870.

Zhang, H., Zhang, H., Luo, J., and Wan, Y. (2019b). Enzymatic cascade catalysis in a nanofiltration membrane: engineering the microenvironment by synergism of separation and reaction. ACS Appl. Mater. Inter. *11*, 22419–22428.

Zhang, Q.M., and Serpe, M.J. (2015). Versatile method for coating surfaces with functional and responsive polymer-based films. ACS Appl. Mater. Inter. *7*, 27547–27553.

STAR★METHODS

KEY RESOURCES TABLE

REGENT or RESOURCE	SOURCE	IDENTIFIER
Chemicals, proteins, and membrane		
N-isopropylacrylamide (NIPAM)	Aladdin	CSA: 2210-25-5
Tris(hydroxymethyl)ainomethane	Aladdin	CSA:77-86-1
N, N, N′, N′-tetramethylethylenediamine (TEMED)	Aladdin	CSA:110-18-9
Polyethyleneimine (PEI 10000Da)	Aladdin	CSA:9002-98-6
Tert-butyl hydroperoxide (tBuOOH)	Macklin	CSA:75-91-2
Ammonium persulfate (APS)	Macklin	CSA:7727-54-0
N,N′-methylenebis(acrylamide) (BIS)	J&K Chemical	CSA:110-26-9
Bisphenol A (BPA, 96%)	J&K Chemical	CSA:80-05-7
Acetic acid	Beijing Chemical Works	CSA:64-19-7
Hydrochloric acid	Beijing Chemical Works	CSA:7647-01-0
Ethanol	Beijing Chemical Works	CSA:64-17-5
Sodium acetate	Sinopharm Chemical Reagent	CSA:127-09-3
Laccase (EC 1.10.3.2, 60-70 kDa, 0.53U mg^{-1})	Sigma-Aldrich	CSA:80498-15-3
Bradford reagent	Sigma-Aldrich	N/A
Dopamine hydrochloride	Sigma-Aldrich	CSA:62-31-7
NF270 membrane	DOW-FILMTEC Co.	N/A

RESOURCE AVAILABILITY

Lead contact

All requests for additional information and reagents should be directed to the Lead Contact, Jianquan Luo (jqluo@ipe.ac.cn).

Materials availability

This study did not generate new unique reagents.

Data and code availability

All data reported in this paper will be shared by the lead contact upon request. This study did not generate any data sets or code. Any additional information required to reanalyze the data reported in this paper is available from the lead contact upon request.

METHOD DETAILS

Microgel synthesis and characterization

PNIPAM microgels synthesis. NIPAM (1.6 g), BIS (0.065 g) and APS (0.035 g) were dissolved in 100 mL deionized water and then transferred to a three-necked round bottom flask equipped with a reflux condenser, a mechanical agitator and nitrogen inlet. The mixed solution was treated with a gentle stream of nitrogen for 30 min and subsequently heated to 70°C to react for 4 h under a gentle stream of nitrogen. After the completion of the reaction, the dispersion of the obtained PNIPAM microgels were purified by repeat centrifugation at 14,000 rpm for 30 min and further purified by dialyzing against water using dialysis tubing (Cellulose membrane, molar weight cut-off (MWCO) = 12,000 Da) for 1 week at room temperature. Finally, the purified microgels were lyophilized by a vacuum freezing dryer.

PNIPAM-PEI microgels synthesis. The cationic thermo-responsive PNIPAM-PEI microgels were synthesized via graft copolymerization of NIPAM and BIS from PEI. Briefly, NIPAM (1.6 g) and BIS (0.16 g) were dissolved in 100 mL deionized water and then transferred to a three-necked round bottom flask. The mixed

solution was treated with a gentle stream of nitrogen for 30 min. PEI (0.8 g, 50 mL) solution was dissolved in water and then neutralized to pH 7 using 1 M HCl solution. Subsequently, PEI solution was added into the flask (total volume was 150 mL) and heated to 70°C under a gentle stream of nitrogen. After reaching the desired temperature, the diluted tBuOOH solution in deionized water (1 mL, 10 mM) was added dropwise to the mixture to initiate the polymerization reaction. The reaction was allowed to proceed for 2 h, at 70°C with constant stirring (300 rpm) under nitrogen atmosphere. After the completion of the reaction, the synthesized PNIPAM-PEI microgels were purified and treated with the same procedure in PNIPAM microgels synthesis section.

Characterization of the microgels. A field emission scanning electron microscopy (FESEM, JSM-7001F, Hitachi) was used to characterize the morphology of the vacuum dried microgels on a thin foil paper. The dynamic light scattering (DLS) measurements under different temperatures were performed for the microgel to analyze the particle size and its temperature responsive behavior. Zeta potential measurements were also carried out to identify the surface charge of the microgel. Both DLS and zeta potential were tested by Zetasizer Nano ZS (Malvern Instruments, U. K.).

Adsorption experiment. Laccase solution (10 mL, 1 g L^{-1}) and BPA solution (40 mL, 10 mg L^{-1}) were first respectively mixed with PNIPAM dispersion (10 mL, 1 g L^{-1}) and then put into the shaker with gently shaking (100 rpm). 2 mL sample solution was taken out every 1 h and centrifuged at 15,000 rpm for 15 min. The supernate was collected. The enzyme activity of the supernate was tested by monitoring the oxidation rate of DMP (10 mM, pH 5) over 1.5 min which was determined by recording the absorbance change at 468 nm using a spectrophotometer. 1 mL DMP solution was added to a cuvette and then 1 mL sample solution was added into the cuvette. The absorbance change was recorded every 15 s. The enzyme activity could be derived by Equation (1) and expressed in μM_{DMP} min^{-1}. The cuvette used in this experiment had an effective length of 1 cm.

$$\text{Enzyme Activity} = \frac{Abs_{min}}{\varepsilon_{468}} \quad \text{(Equation 1)}$$

where, Abs_{min} is the absorbance per minute which is obtained from the slope of the initial linear portion of the kinetic curve (absorbance vs time), ε_{468} is the DMP molar absorption coefficient (ε_{468} = 49,600 $(M\ cm)^{-1}$). Based on the standard curve between enzyme activity and enzyme concentration, the laccase adsorbed on microgels can be calculated. Laccase and PNIPAM solutions were prepared in acetic acid buffer (pH 5, 10 mM).

BPA concentration in the supernate was quantified by high performance chromatography (HPLC, Shimadzu Co. Japan), thereby the amount of BPA adsorbed on PNIPAM microgels can be derived. BPA and PNIPAM solutions were prepared in acetic acid buffer (pH 5, 10 mM). HPLC was installed with two pumps, a UV-visible detector, an automatic sampler, a column oven and a C18 HPLC column (ZORBAX SB-C18, 250 mm × 4.6 mm i.d.; 5 μm; Agilent, USA). HPLC analytic conditions are set as follows: isocratic elution with 50% ultrapure water and 50% HPLC-grade acetonitrile (V/V); flow rate of the mobile phase is 1 mL min^{-1}; injection volume of the sample is 50 μL; the column oven temperature is set at 40°C; samples were detected at 278 nm and one sample took 15 min. The BPA retention time was around 5.98 min. The BPA detection limit in HPLC is 10 μg L^{-1}.

The adsorption efficiency of microgels for BPA is calculated by Equation (2).

$$\text{Adsorption efficiency} = \frac{m_{ad}}{m_{total}} \times 100\% \quad \text{(Equation 2)}$$

Where m_{ad} is the amount of BPA adsorbed on/in the microgels, m_{total} is the total amount of the BPA used in this experiment. The adsorption capacity of microgels for BPA is defined as the amount of BPA absorbed on/in one gram of microgels.

BPA removal by free laccase and PNIPAM/laccase mixture. PNIPAM/laccase mixed solution was prepared by adding laccase solution (10 mL, 1 g L^{-1}) into PNIPAM dispersion (10 mL, 1 g L^{-1}) and subsequently shaking (100 rpm) for 1 h. Laccase solution (10 mL, 0.05 g L^{-1}) and PNIPAM/laccase mixed solution (10 mL, 0.5 g L^{-1} laccase) were then added into BPA solutions (40 mL, 10 mg L^{-1}) respectively. 2 mL sample was taken out after a period of time and 1 mL HCl (0.2 M) was subsequently added to stop the enzymatic

reaction in the samples. The sample was then centrifuged at 15,000 rpm for 15 min and the supernate was collected. BPA biodegradation efficiency was expressed by the residual of BPA in the supernate after a period of time. The residual rate of BPA can be calculated by Equation (3).

$$R_{BPA} = \frac{V_s \cdot C_s}{V_f \cdot C_f} \cdot 100\% \quad \text{(Equation 3)}$$

where V_s and C_s are the BPA volume and concentration of the sample, respectively, V_f and C_f are the volume and concentration of the feed solution, respectively. All the solutions were prepared in acetic acid buffer (pH 5, 10 mM).

Preparation and characterization of PNIPAM modified membrane

In situ modification at high temperature (60°C). The pristine NF270 membrane was soaked in 50% ethanol for 10 s and then immersed in deionized water over night to remove protective agent. After the pretreatment, the membrane was placed in a home-made membrane modification cell in reverse mode (support layer facing feed). First, dopamine (DA) solution (10 mL, 2 g L^{-1} in Tris buffer (10 mM, 25°C, pH 8.5)) was poured into the cell with gently shaking (100 rpm) for 2 h forming a polydopamine (PDA) adhesion layer on the inner surface of the support layer. The mixed monomer solution (5 mL) for the synthesis of PNIPAM which had been deoxygenated by N_2 for 1h was then added into the cell to react at 60°C in the N_2-filled closed environment for 2 h with gently shaking (120 rpm). PNIPAM microgels would *in situ* grow and be confined in the support layer of the NF membrane, thereby accomplishing the membrane modification. The mixed monomer solution consists of NIPAM, BIS and APS, thereinto the concentration of NIPAM was 0.2, 1, 5wt%, respectively, the mass of BIS is 3 mol% of NIPAM, and the mass of APS was 1 mol% of NIPAM. The fabricated PNIPAM-modified NF membrane was soaked in deionized water and shaken (120 rpm) for 12 h to remove unreacted monomers and unstable microgels. According to the difference in NIPAM concentration, PNIPAM-modified NF membranes were named by H-0.2wt%、H-1wt% and H-5wt%.

In situ modification at room temperature (25°C). In this part, the pretreatment and DA coating steps are the same as before. After DA coating, the deoxygenated reaction mixture (5wt% NIPAM, BIS 3 mol% of NIPAM, APS 1 mol% of NIPAM, 5 mL) was added into the cell and another 10 μL TEMED was then added to trigger the decomposition of the initiator at room temperature. *In situ* modification was carried out at room temperature (25°C) in the N_2-filled closed environment with gently shaking (120 rpm) for 0.5, 1 and 2 h, respectively. The fabricated PNIPAM-modified NF membrane was soaked in deionized water and shaken (120 rpm) for 12 h to remove unreacted monomers and unstable microgels. According to the difference in modification time, PNIPAM-modified NF membranes were named by R-0.5 h, R-1 h and R-2 h.

Co-deposition method. After the pretreatment, the membrane was placed on the dead-end filtration cell in reverse mode (own support layer facing feed with an extra polypropylene support between the skin layer and the membrane holder). The mixed solution (10 mL) of dopamine (2 g L^{-1} in Tris buffer (50 mM, 25°C, pH = 8.8)) and PNIPAM-PEI microgels (2 g L^{-1} in Tris buffer) was then poured into cell and allowed to modify the membrane support layer with an agitation of 100 rpm for 1, 2, 4 h, respectively. Finally, the modified membrane was washed with deionized water for several hours to remove unbounded PNIPAM-PEI microgels. According to the difference in modification time, the prepared membranes were named by PEI-1h, PEI-2h, and PEI-4h.

Membrane characterization. FESEM (JSM-7001F, Hitachi) was used to characterize the morphology of the support layer of the PNIPAM modified membranes. Zeta potential of the support layer of the PNIPAM modified membranes as a function of pH was measured by the SurPASS Anton Paar analyser. The testing pH (3–10) of the KCl (1 mM) solution was adjusted with HCl and NaOH solutions. The contact angle of the support layer was determined by using a water drop shape system (OCA20, Dataphysics, Germany).

Membrane water permeability. The permeability (L_p) of the membranes before and after modification was measured by deionized water, which can be derived by Equation (4).

$$L_p = \frac{V_p}{t \cdot A_m \cdot TMP} \quad \text{(Equation 4)}$$

here, V_p is the permeate volume after a certain time, A_m is the effective filtration area (13.4 cm^2) and TMP is the transmembrane pressure.

Preparation and characterization of biocatalytic nanofiltration membranes (BNMs)

The low critical transition temperature (LCST) of PNIPAM microgels is around 32°C. Considering the thermal stability of the NF membrane and laccase, we chose 38°C for laccase immobilization. At 38°C, the PNIPAM microgels are in a collapsed state, and the resulting larger pore size of the support layer has low geometric confinement to laccase, thus making it easier for laccase embedding into the membrane by reverse filtration. After reverse filtration of laccase, the operating temperature was kept at 25°C and the membrane was washed with acetic buffer to remove weekly confined laccase. The PNIPAM microgel is in a swollen state at 25°C, and thus the pores of the support layer would be narrowed which can effectively confine laccase in the membrane. The detailed preparation procedure was as follows:

The PNIPAM modified membranes were first placed in the dead-end filtration cell under reverse mode. The dead-end filtration cell was then placed in a water bath. Acetic buffer (pH = 5, 10 mM) was used to equilibrate the membranes for 20 mins at 2 bar at 38°C. After that, 45 mL laccase solution (0.5 g L^{-1} in acetic buffer, pH = 5, 100 rpm) was added into the cell and reversely filtrated into the support layer of the PNIPAM modified membranes at 38°C, at 2 bar until 43 mL permeate was collected for enzyme loading analysis. Then 10 mL acetic buffer (pH = 5,10 mM) was added into the cell to wash the enzyme-loaded membrane at 2 bar at room temperature (25°C). 2 mL retentate and 10 mL washing residual were collected together for enzyme loading analysis. The obtained BNMs were then washed with acetic buffer (20 mL, 2 bar, pH = 5) in normal mode (skin layer facing feed) to remove the weekly adsorbed laccase at 25°C. This washing solution (20 mL) was collected for enzyme loading analysis. After washing, the BNMs were soaked in acetic buffer (10 mL, 10 mM, pH = 5) at 4°C overnight. Finally, the laccase-loaded membranes were put in the cell under normal mode, and 10 mL acetic buffer was used to wash the membranes again at 2 bar at 25°C. The soaking and washing solutions (total 20 mL) were mixed and collected for analysis.

The BNMs prepared with the PINPAM modified NF membranes by in-situ method at high temperature (60°C) were termed as H-0.2wt%-E, H-1wt%-E and H-5wt%-E respectively according to the different NIPAM monomer concentration. The BNMs prepared with the PINPAM modified NF membranes by in-situ method at room temperature (25°C) were termed as R-0.5h-E, R-1h-E and R-2h-E respectively according to the different modification time. The BNMs prepared with PNIPAM-PEI modified membrane were termed as PEI-1h-E, PEI-2h-E and PEI-4h-E respectively according to the different modification time. Their water permeability was also tested and calculated by Equation (3).

Enzyme loading efficiency. Bradford method was used to measure the protein concentration of the samples. The sample (1 mL) which was taken from enzyme solution was mixed with 1 mL Bradford assay. After 5 mins, the absorbance at 595 nm was recorded. The detection limit of protein with this method was 20 μg L^{-1}. According to the mass balance, the amount of immobilized protein can be calculated by Equation (5).

$$M_{IMM} = C_f \cdot V_f - C_p \cdot V_p - C_R \cdot V_R - C_W \cdot V_W - C_{SW} \cdot V_{SW} \quad \text{(Equation 5)}$$

where M_{IMM} is the amount of immobilized protein, C_f, C_p, C_R, C_W, C_{SW} are the protein concentrations in the feed, permeate, retentate and washing residual, washing solutions in normal mode, and the mixture of soaking and washing solution, respectively. V_f, V_p, V_R, V_W, V_{SW} are volumes of the feed (45 mL), permeate (43 mL), retentate and washing residual (12 mL), washing solutions in normal mode (20 mL), and the mixture of soaking and washing solution (30 mL), respectively. The loading efficiency is expressed as Equation (6).

$$\text{Loading efficiency} = \frac{M_{IMM}}{C_f V_f} \times 100\% \quad \text{(Equation 6)}$$

BPA removal efficiency and reusability of the BNM. The performance of the BNMs was evaluated by the removal of a representative OMPs, BPA. BPA would cause reproductive, immunity, neurological, and metabolic diseases. BPA solution used in this study was prepared by acetic buffer (10mM, pH = 5.0) with a concentration of 10 mg L^{-1}. BPA solution (18 mL) was added into the cell for filtration, where the permeate flux was kept constant at 7.46 L m^{-2} h^{-1} by manually controlling the operating pressure. Permeate (15 mL) was collected and mixed with HCl solution (7.5 mL, 0.2 M) to terminate the enzymatic reaction. To evaluate its reusability, each BNM was reused for 4 times. After each experiment, the membranes were washed with acetic buffer (10 mM, pH = 5) under stirring (300 rpm) in an open cell for 20 min and then in flow through mode for 10 mins to remove the adsorbed BPA and its products on/in the membrane. Finally, they were soaked in acetic buffer (10 mM, pH = 5) at 4°C overnight. The BPA removal efficiency (X_{BPA}) can be derived by Equation (7).

$$X_{BPA} = \left(1 - \frac{C_p}{C_f}\right) \times 100\% \quad \text{(Equation 7)}$$

where C_p and C_f are the concentrations of BPA in permeate and feed, respectively.

Mechanism analysis of BPA removal efficiency decline during reuse

The catalytic efficiency decline of the PNIPAM-based BNMs caused by enzyme leakage and products accumulation were evaluated as follows.

Products accumulation. The degradation mechanism and products identification of BPA by laccases have been investigated by numerous studies. It suggested that during the reaction between BPA and laccase, low molecular weight (LMW) products such as phenol and 4-isopropenylphenol was first formed. Then high molecular weight (HMW) polymers were formed by further condensation reaction of BPA, 4-isopropenylphenol, and 4-hydroxy-isopropenylphenol. Therefore, for BNMs, the longer residence time of products in the membrane, the more HMW products would be produced which were more likely to accumulate in the membrane. In our studies, by means of HPLC analysis, 2 peaks with shorter retention time than BPA were identified in BPA degradation permeate, indicating LMW products were produced after the treatment by BNMs. We named these two LMW products as product (I) and (II). Herein, to evaluate the products accumulation degrees of the PNIPAM-based BNMs, the variations of the ratio of product (I) to degradation products in the permeate was measured after each reuse cycle.

Enzyme leakage. To evaluate the enzyme leakage of the PNIPAM-based BNMs, we used acetic acid buffer (pH 5, 10 mM) to wash the BNM at a constant permeate flux kept of 7.46 L m-2 h-1 at 25°C. Except without adding BPA, all the conditions in this experiment were the same as BPA removal experiment.

Regeneration of the BNM

When the membrane performance cannot meet the demands, the BNMs needed to be regenerated by elution-cleaning-reloading processes. First, laccase was eluted from the membrane by eluting solution (deionized water and pH 10 NaOH solution) with a constant pressure of 4 bar at 38°C. The eluted solution was collected and the amount of leaked enzyme was tested. Then the membrane was soaked in deionized water for 12 h and shaken at 120 rpm. Subsequently, the cleaned membrane was reloaded with fresh laccase to reconstruct the BNMs.